CERN-INTC-2020-064 / INTC-P-579
22/09/2020

EUROPEAN ORGANIZATION FOR NUCLEAR RESEARCH

Proposal to the ISOLDE and Neutron Time-of-Flight Committee

Probing the magicity and shell evolution in the vicinity of $N = 50$ with high-resolution laser spectroscopy of ^{81,82}Zn isotopes

September 22, 2020

M. Athanasakis,[1,2] S. W. Bai,[3] S. Bester,[4] M. L. Bissell,[5,6] T. E. Cocolios,[1] A. de Bruyn,[4] R. P. de Groote,[7] C. Duchemin,[1,6] K. T. Flanagan,[5,8] S. Franchoo,[9] R. F. Garcia Ruiz,[10] S. Geldhof,[1] R. Heinke,[1] J. Johnson,[1] Á. Koszorús,[11] Y. C. Liu,[3] G. Neyens,[1,2] F. P. Gustafsson,[1] C. M. Ricketts,[5] S. Rothe,[6] C. M. Steenkamp,[4] D. Verney,[9] A. R. Vernon,[10] S. J. Wang,[3] F. J. Waso,[4] S. G. Wilkins,[10] W. Wojtaczka,[1] X. F. Yang[3]

[1] *KU Leuven, Instituut voor Kern- en Stralingsfysica, B-3001 Leuven, Belgium*
[2] *Experimental Physics Department, CERN, CH-1211 Geneva 23, Switzerland*
[3] *School of Physics and State Key Laboratory of Nuclear Physics and Technology, Peking University, Beijing 100871, China*
[4] *Laser Research Institute, Stellenbosch University, 7600, Stellenbosch, South Africa*
[5] *School of Physics and Astronomy, The University of Manchester, Manchester M13 9PL, United Kingdom*
[6] *Engineering Department, CERN, CH-1211 Geneva 23, Switzerland*
[7] *Department of Physics, University of Jyväskylä, PB 35(YFL) FIN-40351 Jyväskylä, Finland*
[8] *Photon Science Institute Alan Turing Building, University of Manchester, Manchester M13 9PY, United Kingdom*
[9] *Institut de Physique Nucléaire Orsay, IN2P3/CNRS, 91405 Orsay Cedex, France*
[10] *Massachusetts Institute of Technology, Cambridge, MA 02139, USA*
[11] *Department of Physics, University of Liverpool, Liverpool L69 7ZE, United Kingdom*

Spokesperson: X.F. Yang, xiaofei.yang@pku.edu.cn
Co-spokesperson: T.E. Cocolios, thomas.elias.cocolios@cern.ch
Local contact person: S. Geldhof, sarina.geldhof@kuleuven.be

Abstract: We propose to measure the ground state properties of ^{81,82}Zn ($Z = 30$) using the Collinear Resonance Ionization spectroscopy (CRIS) method. This measurement will allow an unambiguous assignment of the ground state spin of ^{81}Zn ($N = 51$), aiming to study the evolution and the predicted inversion of neutron single-particle orbits above $N = 50$, when approaching ^{78}Ni. The measured nuclear electromagnetic moments will help to identify the ground state configuration and structure of the ^{81}Zn, while the nuclear charge radii up to ^{82}Zn and the odd-even staggering, 2 neutrons above $N = 50$, will provide a sensitive probe of the magic nature of $N = 50$ near ^{78}Ni.

Requested shifts: 16 shifts of radioactive beam and 2 shifts of stable beam (1 run)

1 Scientific context

1.1 The vicinity of $Z = 28$ and $N = 50$

Magic nuclei are the corner stones of our understanding of nuclear structure. While they are well established close to the valley of stability, they are under question in regions with extreme proton-to-neutron ratio. In particular, the region of ^{78}Ni with $Z = 28$ and $N = 50$, with 14 neutrons in excess from the heaviest stable nickel isotope, and 6 β-decays away from the stable ^{78}Se, is the subject of scrutiny by the nuclear physics community. The isotope ^{78}Ni is itself very difficult to be produced with sufficient yield at current radioactive beam facilities to allow for detailed measurements of its ground state (g.s.) properties.

As a consequence, most of these studies have been performed with other proxies, such as the copper isotopes with $Z = 29$ [1]. The study of the low-lying structure across these odd-A isotopes has shown a steady migration of the single-particle energy levels [2], as measured by the nuclear spin and electromagnetic moments of the g.s. of copper and gallium isotopes [3, 4, 5]. While this first observation might suggest a structural change close to $Z = 28$, the comparison with the different models actually highlights how robust the underlying $Z = 28$ structure remains. This is further confirmed from the observation of the binding energies up to ^{79}Cu. Amongst all the neutron-rich $N = 50$ isotones, copper shows an increased binding that suggests the trend will coincide with a doubly magic system in ^{78}Ni [6]. Only very recently could the the first excited state in ^{78}Ni be established at RIBF-RIKEN via in beam γ-spectroscopy [7]. Although this experiment provided an evidence of the doubly magic nature of ^{78}Ni, it also suggested a deformed state at low energy. This result potentially echoes the earlier observation of shape coexistence appearing in ^{79}Zn ($N = 49$) and ^{80}Ge ($N = 48$) [8, 9], and is in line with the prediction of shape coexistence by large-scale shell-model calculations [10]. A breakdown of the proton $Z = 28$ shell closure above $N = 50$ is predicted, that favours deformed ground states for more exotic nickel isotopes [7]. As these neutron-rich nickel isotopes are not yet accessible at current radioactive beam facilities, we propose to study the ground state structure of the $N = 51$ isotope ^{81}Zn, the closest even-Z isotope to ^{79}Ni. Through high-resolution laser spectroscopy, we can measure directly the g.s. spin, while the moments will reveal information on the single particle (or collective) nature of this state. The mean square charge radii up to ^{82}Zn will allow to probe the magic character of the $N = 50$ gap by investigating the kink at the magic number.

1.2 The zinc isotopes

1.2.1 Shell evolution of $N = 51$ isotones: nuclear spin of ^{81}Zn:

For $N = 51$ isotones, one neutron above the $N = 50$ shell closure, the spin/parity of g.s. $5/2^+$ and first excited state $1/2^+$ are known experimentally from $Z = 40$ down to $Z = 32$ (Fig. 1) [11, 12], with a dramatic drop in energy of the $1/2^+$ state. This reduction in energy difference between the $1/2^+$ and $5/2^+$ states can be attributed to the effect of the tensor component of the monopole interaction on the $d_{5/2}$ orbit within the shell-

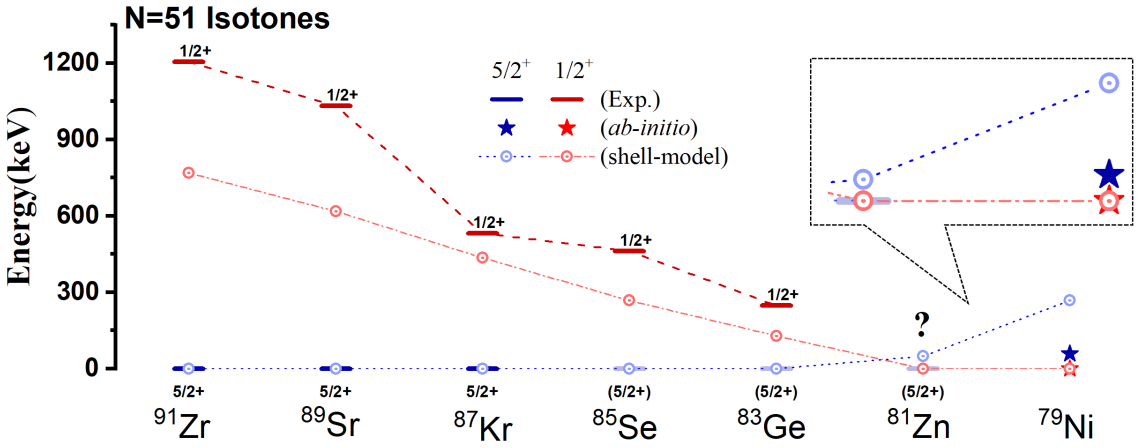

Figure 1: $1/2^+$ and $5/2^+$ energy levels for $N = 51$ isotones compared with the theoretical calculations.

model framework [13, 14, 15]. The $1/2^+$ level is predicted to become the g.s. in ^{81}Zn and ^{79}Ni from a shell-model calculation using jj45pna [16] (see Fig. 1). Moreover, the $5/2^+$ and $1/2^+$ levels in ^{81}Zn are predicted to be nearly degenerate. An *ab-initio* coupled-cluster calculation including the continuum also predicted an inversion of the $5/2^+$ and $1/2^+$ states in ^{79}Ni [17]. A direct experimental assignment of the g.s. spin of ^{81}Zn and ^{79}Ni is thus highly motivated but currently impossible for ^{79}Ni. For ^{81}Zn, however, the production yield is sufficient at ISOLDE to perform a direct spin measurement using the collinear resonance ionization laser spectroscopy (CRIS) method [4].
Multiple experimental proposals [13, 14] and investigations [18] have been motivated and performed at ISOLDE in order to determine (indirectly) the spins of the low-lying states of ^{81}Zn, but until now, the g.s. spin of ^{81}Zn remains controversial [18]. High-resolution laser spectroscopy is the only method that allows for a direct measurement of the ^{81}Zn g.s. spin, and it is currently only possible at ISOLDE, thanks to the high sensitivity offered by the CRIS method.

1.2.2 Nuclear moments of ^{81}Zn*:*

This predicted $1/2^+$ g.s. in ^{79}Ni and ^{81}Zn may come from a single neutron in the $3s_{1/2}$ orbit or have a rather mixed configuration, e.g., with $[2^+ \otimes d^1_{5/2}]1/2^+$. The nuclear magnetic moment is a sensitive probe of the wave-function in near-magic isotopes. The quadrupole moment can also reflect the single-particle effect or configuration mixing. Therefore, to study experimentally the evolution or inversion of $\nu 3s_{1/2}$ and $\nu 2d_{5/2}$ orbits above $N = 50$, the nuclear spin and the moment measurements of ^{81}Zn are essential. These results will also provide stringent tests for recently developed large-scale shell model [19] and microscopic *ab-initio* [17] calculations.

1.2.3. Nuclear charge radii of zinc isotopes beyond $N = 50$*:*

Approaching $Z = 28$ and above $N = 50$, the charge radii data are very limited (Fig. 2). The closest isotope to $Z = 28$ with a measured radius beyond $N = 50$ is ^{82}Ga ($N = 51$)

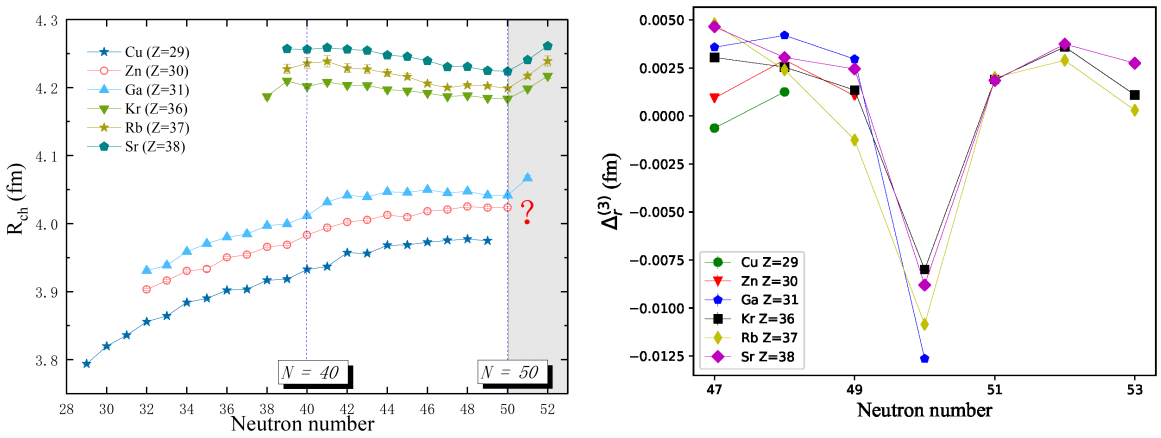

Figure 2: (Left): Experimental charge radii in the nickel region. (Right): Odd-even staggering of isotopes around $N = 50$. The statistical errors are not included in the plot for a better visualization.

[20, 21]. For the nickel isotopes, results from measurements up to $N = 42$ [22] are currently being analyzed and these could be extended at most up to $N = 44$ using the CRIS method. Recent charge radii measurements of copper isotopes up to $N = 49$ [1] and zinc isotopes up to $N = 50$ [19] have provided prominent tests for *ab-initio* and density functional calculations, which were applied in this mass region for the first time [1], as well as for shell-model calculations [19]. The magic shell effect can be identified by the characteristic kink in the charge radii of isotopes beyond $N = 50$, as seen in the krypton, rubidium, strontium and gallium isotopes (Fig. 2 (Left)). This magic effect can be better observed as a local inversion of the odd-even staggering (OES) ($\Delta^{(3)}_{1n} r = \frac{1}{2}(-1)^{N+1}[r_{N+1} - 2r_N + r_{N-1}]$[21]), as seen in Fig. 2 (Right), which seems to increase in gallium. In order to investigate how the shell gap effect evolves towards $Z = 28$, we aim to measure the charge radii of ^{81,82}Zn. This measurement will also provide a further test of the state-of-the-art nuclear theories [1].

In summary, in this proposal, we shall perform high-resolution laser spectroscopy measurements of ^{81,82}Zn isotopes to address the following questions:
1. What is the g.s. spin in ^{81}Zn (evolution of $1/2^+$ level in $N = 51$ isotones)?
2. Is the g.s. of ^{81}Zn a single-particle state?
3. How does the charge radii trend and the local OES behave above $N = 50$?

2 Experimental method

2.1 Beam production and yields

Zinc beams can be produced by impinging the 1.4 GeV proton onto a UCx target and then laser-ionized with the RILIS. The zinc beam production rates are well known and documented at ISOLDE. Experimental yields have been measured up to ^{81}Zn, see Table 1. The yield for ^{82}Zn has been determined from the ActiWiz in-target production

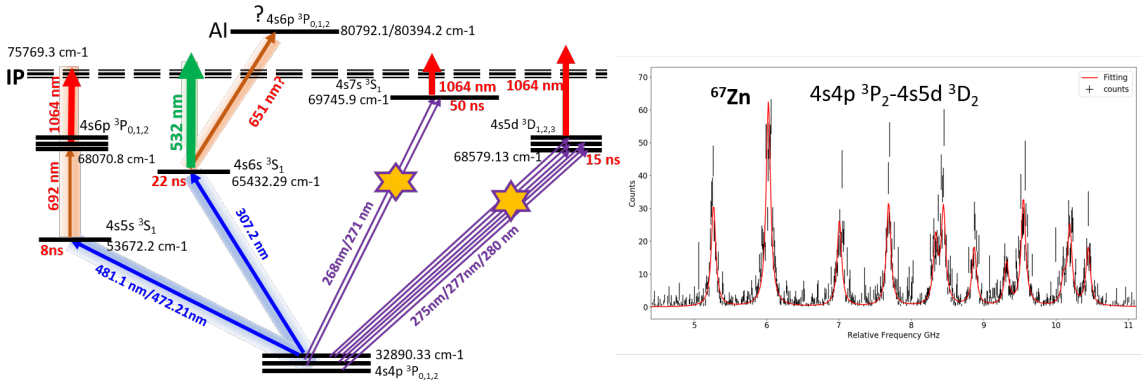

Figure 3: (Left): Laser resonant ionization schemes. (Right): Hfs spectra of ^{67}Zn from the offline test.

information, accounting for the trend in release efficiency extrapolated from the $^{77-81}$Zn isotopes with half-lives below 3 s. For a high sensitivity laser spectroscopy measurement, it is important to limit isobaric contaminants if possible against overloading ISCOOL during bunching. In these ^{81,82}Zn beams, near-stability rubidium isotopes appear as the major contaminants. Through the years, many techniques have been used to suppress the rubidium from the zinc beams, such as the use of the proton-to-neutron converter, of a quartz transfer line, or of both combined [23, 24, 25, 26]. In each case, the suppression of rubidium is far superior than the suppression of the zinc beam. When combining the neutron converter and the quartz transfer line, the suppression of the zinc would be too severe. Therefore, we suggest to use the quartz transfer line only. It offers the best compromise in contaminant suppression, yet keeping the yields of the zinc isotopes of interest (^{81,82}Zn) high enough, as shown in the Table I.

2.2 High-resolution CRIS experiment

The zinc beam, after being cooled and bunched in a linear Paul trap (ISCOOL), is delivered to the CRIS experiment. It first passes through a charge exchange cell to be neutralized [27]. A deflector and field ionization unit cleans away remaining ions and highly excited atoms, so that a pure atomic bunch is delivered to the laser-atom interaction region [28], which is maintained at ultra-high vacuum (10^{-10} mbar) to minimize non-resonant collisional ionization. The atom bunch is overlapped in space and in time with the lasers to resonantly excite and ionize the atom. One of the transitions is scanned with a narrowband laser to reveal the hyperfine structure (hfs). The resonantly ionized bunch is then deflected towards an ion detector. The hfs spectrum is reconstructed by counting the ion rate as a function of the laser frequency.

2.3 Zinc ionization scheme

Figure 3 (left) shows possible laser ionization schemes of zinc atoms. The transitions of $^3P_{0,1,2} \rightarrow ^3D_{1,2,3}$ and $^3P_{0,1} \rightarrow ^3S_1$ (marked with stars) have been tested offline with a laser-ablation ion source at CRIS [29] in order to determine the most suitable ionization scheme.

One of the tested schemes ($^3P_2 \rightarrow ^3D_2$), is found to have a good signal-to-background ratio and a good sensitivity of the hfs constants and field shift to the nuclear observables. A well resolved hfs spectrum is observed, as shown in Fig. 3 (right). For this transition, the narrowband laser light at 280 nm could be provided by an injection-seeded laser as used before to study copper [4]. The non-resonant ionization step (1064 nm) can be obtained from a high-power Nd:YAG laser at CRIS.
Another two additional transitions marked with shadow will be tested before the experiment. Our recent investigations have also demonstrated that excitation to Rydberg states just below the IP, followed by field ionization, could lead to a further reduction in collisional background, while maintaining the ionization efficiency [30]. We have investigated preliminary the field ionization of zinc with low-resolution tunable lasers during the offline test, and multiple series of the Rydberg states have been clearly observed. This will also be further tested with high resolution.

2.4 Decay tagging

The neutron-rich zinc isotopes have known isomers as observed in previous studies up to ^{79}Zn [31]. In ^{81}Zn, no isomer has been reported so far, but the discrepancies in the measured half-lives, as well as the diverging interpretations by the different groups who have investigated its decay into ^{81}Ga [18], cannot exclude that this isotope may display isomerism too. At the CRIS experiment, we have demonstrated that laser-assisted radiation detection can be used to study the decay of resonantly-ionized isomers in clean conditions, e.g., using α-decay from neutron-deficient francium isotopes [32, 33, 34]. Moreover, the CRIS decay spectroscopy station has recently been adapted to study the hfs of the exotic ^{52}K isotope via its β-decay [35]. This allowed for a higher sensitivity measurement, as the β-decay detection is not sensitive to the high amount of stable isotopes that were present in this beam. A similar detection strategy can be applied for the short-lived neutron-rich zinc isotopes, in case the background is found to be stable or very long-lived. In a future addendum, a dedicated decay spectroscopy study of the ^{81}Zn g.s. and eventual isomeric state is considered.

2.5 Beam time request

The details of the zinc beam production and the required shifts for this proposal are summarized in Table 1.
In order to have a consistent determination of the charge radii, a few isotopes overlapping with the previous studies [19] have to be measured. We will re-measure the even-even $^{72-80}$Zn (single resonance only) and even-odd ^{79g,m}Zn isotopes. For laser spectroscopy experiments on isotopes with yields above 10^4 pps, the data taking time is mostly determined by the frequency range that has to be scanned to observe all hfs peaks, which depends on the nuclear moments and the atomic hyperfine fields. The frequency range for the hfs spectrum of the ^{67}Zn isotope is $\sim$7 GHz for the most appropriate transitions, based on the offline test and the previous studies at COLLAPS [31]. For ^{79g,m}Zn, 1.5 shifts are needed to scan the 10 GHz frequency range, thus covering the hfs components of the ground and isomeric state [8]. The times are calculated by considering: 10 MHz/step;

Table 1: Zinc yields using protons on target or on converter, without and with a quartz transfer line, and requested shifts. * Only ^{80}Zn has measured yields with protons on target and a quartz transfer line and has been used as a reference to rescale the main yields. Yields with a quartz line are used to estimate the required beam time (taking into account the reduced isobar contamination).

Isotope	$T_{1/2}$ [s]	Yield [μC^{-1}]	Yield [μC^{-1}] with quartz	Yield [μC^{-1}] with converter	Shifts
$^{72-80}$Zn		$> 10^4$	$> 10^4$ *	$> 10^4$	1
^{79g,m}Zn	$0.995/ > 0.2$	$> 10^4$	$> 10^4$ *	$> 10^4$	1.5
^{81}Zn	0.29	5.5×10^3	1.3×10^3 *	7.5×10^2	7
^{82}Zn	0.28	1000	250 *	650	2.5
^{70}Zn	Stable	Reference isotope for isotope shift			4
Total:					**16**
Stable beam: for the optimization of the experimental setup					**2**

15 s/step including 5 s laser stabilization time for each frequency change and three independent hfs measurements. For the even-even $^{72-80}$Zn isotopes, with only 1 resonance in the hfs ($I = 0$), another 1 shift is requested. To measure isotope shifts, each hfs measurement has to be done relative to a reference isotope (typically a $I = 0$ isotope). Therefore, sufficient time for reference isotope measurements is needed, which typically amounts to $25 - 50\%$ of the total beam time (50% when more isotopes are scanned). Therefore, we request 4 shifts for regular measurements on a reference isotope. For the exotic ^{81}Zn isotope, the production yield is 2-3 orders of magnitude lower than the ^{79}Zn and the existence of an isomeric state is not excluded. Thus the hfs should be scanned over a sufficiently large range to cover both a possible $1/2^+$ and $5/2^+$ hfs, estimated to be 10 GHz based on the effective single-particle g-factors of $1/2^+$ and $5/2^+$ states. Due to the low production yield, scans of about 60 s per step (10 MHz/step) and three independent hfs measurements are required in order to obtain sufficient statistics with reliable error determination. Thus, about 7 shifts are requested for the study of ^{81}Zn including 0.5 shift for searching the resonance peaks. The study of ^{82}Zn ($I = 0$) will require only 2.5 shifts because of the single-resonance, although its production is 10 times less than that of ^{81}Zn. Additionally, 2 shifts with stable beam before the run are requested for optimizing the experimental set-up and laser scheme.

Summary of requested shifts: 16 shifts are requested using a UCx target with a quartz transfer line for the study of neutron-rich zinc isotopes. In addition, 2 shifts of stable beam time prior to the online run is requested for the optimization.

References

[1] R. P. de Groote et al. Measurement and microscopic description of odd-even staggering of charge radii of exotic copper isotopes. *Nature Physics*, 16:620–624, 2020.

[2] S. Franchoo, K. Kinglov, Yu. Kudryavtsev, W. F. Mueller, R. Raabe, P. Van Duppen, J. Van Roosbroeck, L. Vermeren, and A. Wöhr. Beta decay of $^{68-74}$Ni and level structure of neutron-rich Cu isotopes. *Physical Review Letters*, 81:3100–3103, 1998.

[3] K. T. Flanagan et al. Nuclear spins and magnetic moments of ^{71,73,75}Cu: inversion of the $\pi 2p_{3/2}$ and $\pi 1f_{5/2}$ levels in ^{75}Cu. *Physical Review Letters*, 103:142501, 2009.

[4] R. P. de Groote et al. Dipole and quadrupole moments of $^{73-78}$Cu as a test of the robustness of the $Z = 28$ shell closure near ^{78}Ni. *Physical Review C*, 96:041302(R), 2017.

[5] B. Cheal et al. Nuclear spins and moments of ga isotopes reveal sudden structural changes between $N = 40$ and $N = 50$. *Physical Review Letters*, 104:252502, 2010.

[6] A. Welker et al. Binding energy of ^{79}Cu: probing the structure of the doubly magic ^{78}Ni from only one proton away. *Physical Review Letters*, 119:192502, 2017.

[7] R. Taniuchi et al. ^{78}Ni revealed as a doubly magic stronghold against nuclear deformation. *Nature*, 569:53–58, 2019.

[8] X. F. Yang et al. Isomer shift and magnetic moment of the long-lived $1/2^+$ isomer in $^{79}_{30}$Zn$_{49}$: signature of shape coexistence near ^{78}Ni. *Physical Review Letters*, 116:182502, 2016.

[9] A. Gottardo and Vothers. First evidence of shape coexistence in the ^{78}Ni region: Intruder 0_2^+ state in ^{80}Ge. *Physical Review Letters*, 116:182501, May 2016.

[10] F. Nowacki, A. Poves, E. Caurier, and B. Bounthong. Shape coexistence in ^{78}Ni as the portal to the fifth island of inversion. *Physical Review Letters*, 117:272501, Dec 2016.

[11] J. S. Thomas, D. W. Bardayan, J. C. Blackmon, J. A. Cizewski, U. Greife, C. J. Gross, M. S. Johnson, K. L. Jones, R. L. Kozub, J. F. Liang, R. J. Livesay, Z. Ma, B. H. Moazen, C. D. Nesaraja, D. Shapira, and M. S. Smith. First study of the level structure of the r-process nucleus ^{83}Ge. *Physical Review C*, 71:021302, Feb 2005.

[12] S. Padgett et al. β decay of ^{81}Zn and migrations of states observed near the $N = 50$ closed shell. *Physical Review C*, 82:064314, Dec 2010.

[13] Mathieu Babo. Spectroscopy of ^{81}Zn populated via one-neutron transfer ^{80}Zn(d,p) using actar tpc. *(CERN-INTC-2017-011.INTC-P-494)*, January 2017.

[14] Riccardo Orlandi et al. Spectroscopy of low-lying single-particle states in ^{81}Zn populated in ^{80}Zn(d,p) reaction. *(CEN-INTC-2012-051, INTC-P-352)(CERN-INTC-2020-004.INTC-SR-099)*, January 2020.

[15] K. Sieja, F. Nowacki, K. Langanke, and G. Martínez-Pinedo. Shell model description of zirconium isotopes. *Phys. Rev. C*, 79:064310, Jun 2009.

[16] K. Maurya, P. C. Srivastava, and I. Mehrotra. Shell model description of $N = 51$ isotones. *IOSR Journal of Applied Physics*, 3:52, 2013.

[17] G. Hagen, G. R. Jansen, and T. Papenbrock. Structure of ^{78}Ni from first-principles computations. *Physical Review Letters*, 117:172501, Oct 2016.

[18] V. Paziy et al. Fast-timing study of ^{81}Ga from the β decay of ^{81}Zn. *Physical Review C*, 102:014329, Jul 2020.

[19] L. Xie et al. Nuclear charge radii of $^{62-80}$Zn and their dependence on cross-shell proton excitations. *Physics Letters B*, 797:134805, 2019.

[20] B. Cheal et al. Laser spectroscopy of gallium isotopes beyond $N = 50$. *Journal of Physics: Conference Series*, 381:012071, 2012.

[21] G. J. Farooq-Smith et al. Probing the $_{31}$Ga ground-state properties in the region near $Z = 28$ with high-resolution laser spectroscopy. *Physical Review C*, 96:044324, 2017.

[22] B. Cheal et al. High-resolution laser spectroscopy of nickel isotopes. *(CERN-INTC-2013-007.INTC-P-373)*, May 2013.

[23] J. Van de Walle et al. Coulomb excitation of neutron-rich Zn isotopes: first observation of the 2_1^+ state in ^{80}Zn. *Physical Review Letters*, 99:142501, 2007.

[24] E. Boucquerel, R. Catherall, M. Eller, S. Marzari, and T. Stora. Purification of a Zn radioactive ion beam by alkali suppression in a quartz line target prototype. *European Physical Journal: Special Topics*, 150:277–280, 2007.

[25] J. Van de Walle et al. Coulomb excitation of neutron-rich Zn isotopes: first observation of the 2_1^+ state in ^{80}Zn. *Physical Review C*, 79:014309, 2009.

[26] V. Paziy et al. Fast-timing study of ^{81}Ga from the β decay of ^{81}Zn. *Physical Review C*, 102:014329, 2020.

[27] A. R. Vernon et al. Simulation of the relative atomic populations of elements $1 \leq Z \leq 89$ following charge exchange tested with collinear resonance ionization spectroscopy of indium. *Spectrochemica Acta B*, 153:61–83, 2019.

[28] A. R. Vernon et al. Optimising the collinear resonance ionisation spectroscopy (CRIS) experiment at CERN-ISOLDE. *Nuclear Instruments and Methods in Physics Research B*, 463:384–389, 2020.

[29] R. F. Garcia Ruiz et al. High-precision multiphoton ionization of acceleracted laser-ablated species. *Physical Review X*, 8:041005, 2018.

[30] A. R. Vernon et al. Laser spectroscopy of indium Rydberg atom bunches by electric field ionization. *Nature Scientific Reports*, 10:12306, 2020.

[31] C. Wraith et al. Evolution of nuclear structure in neutron-rich odd-Zn isotopes and isomers. *Physics Letters B*, 771:385–391, 2017.

[32] K. M. Lynch et al. Decays-assisted laser spectroscopy of neutron-deficient francium. *Physical Review X*, 4:011055, 2014.

[33] K. M. Lynch et al. Combined high-resolution laser spectroscopy and nuclear decay spectroscopy for the study of low-lying states in ^{206}Fr, ^{202}At, and ^{198}Bi. *Physical Review C*, 93:014319, 2016.

[34] G. J. Farooq-Smith et al. Laser and decay spectroscopy of the short-lived isotope ^{214}Fr in the vicinity of $N = 126$ shell closure. *Physical Review C*, 94:054305, 2016.

[35] Á. Koszorús et al. Charge radii of exotic potatssium isotopes challenge nuclear theory and the magic number character of $N = 32$. *Nature Physics*, under:review, 2020.

Appendix

DESCRIPTION OF THE PROPOSED EXPERIMENT
The experimental setup comprises: (*name the fixed-ISOLDE installations, as well as flexible elements of the experiment*)

Part of the	Availability	Design and manufacturing
CRIS	☒ Existing	☒ To be used without any modification

HAZARDS GENERATED BY THE EXPERIMENT Hazards named in the document relevant for the fixed CRIS installation.